2019

Molecular Level Comparison of Water Extractives of Maple and Oak with Negative and Positive Ion ESI FT-ICR Mass Spectrometry

Zhongqi He

Rachel L. Sleighter

Patrick G. Hatcher

Shasha Liu

Fengchang Wu

See next page for additional authors

Authors

Zhongqi He, Rachel L. Sleighter, Patrick G. Hatcher, Shasha Liu, Fengchang Wu, Haixuan Zou, and O. Modesto Olanya

He Zhongqi (Orcid ID: 0000-0003-3507-5013)

Molecular level comparison of water extractives of maple and oak with negative and positive ion ESI FT-ICR mass spectrometry

Zhongqi He [a,*], Rachel L. Sleighter [b], Patrick G. Hatcher [b], Shasha Liu [c], Fengchang Wu [c], Haixuan Zou [d], and O. Modesto Olanya [e]

[a] Southern Regional Research Center, USDA Agricultural Research Service, 1100 Robert E. Lee Blvd., New Orleans, LA 70124, USA

[b] Department of Chemistry and Biochemistry, Old Dominion University, Norfolk, VA 23529, USA

[c] State Key Laboratory of Environmental Criteria and Risk Assessment, Chinese Research Academy of Environmental Sciences, Beijing 100012, China

[d] Department of Chemical and Biological Engineering, the University of Maine, Orono, ME 04469, USA

[e] Eastern Regional Research Center, USDA Agricultural Research Service, 600 East Mermaid Lane, Wyndmoor, PA 19038, USA

* Corresponding author, phone 504-286-4516, zhongqi.he@ars.usda.gov

This article has been accepted for publication and undergone full peer review but has not been through the copyediting, typesetting, pagination and proofreading process which may lead to differences between this version and the Version of Record. Please cite this article as doi: 10.1002/jms.4379

Abstract

Soluble extractives in wood function to protect living trees from destructive agents and also contribute to wood color and fragrance. Some extractive components have biological activities with medical applications. They also play important roles in wood processing and related applications. To increase the knowledge of wood chemistry, maple and oak were extracted by water. Ultraviolet/visible (UV/vis) spectroscopy indicated the presence of a phenolic compound, resorcinol, in maple extractives having higher molecular mass and more aromatic components than oak extractives. Negative and positive electrospray ionization Fourier transform ion cyclotron resonance mass spectrometry (ESI FT-ICR-MS) identified thousands of formulas in the two samples in the m/z range of 200-800. They mainly fall into the lignin-, carbohydrate- and tannin-like compound categories. The top 25 peaks (i.e., formulas) with the highest relative magnitude in negative ESI represented nearly 50% of the summed total spectral magnitude of all formulas assigned in the maple and oak extractives. Furthermore, the base peak (i.e., most abundant peak) accounted for about 14% of the total abundance in each wood sample. Literature comparisons identified 17 of 20 formulas in the top 5 peaks of the four spectra as specific bioactive compounds in trees and other plants, implying the potential to explore utilization of maple and oak extractives for functional and medicinal applications. The various profiling of the top 25 peaks from the two samples also suggested the possible application of FT-ICR-MS for detecting chemical markers useful in profiling and identification of wood types and sources.

Keywords: Fourier transform ion cyclotron resonance mass spectrometry, maple, oak, van Krevelen diagrams

1. Introduction

Besides cellulose, hemicellulose, and lignin as the main structure components of cell walls, wood contains other non-structural substances known as extractives [1, 2]. Wood extractives may be extracted by water and/or organic solvents. Extractives in wood function to protect living trees from destructive pest agents and contribute to wood color and fragrance. Some extractive components show specific biological activities with medical applications [3]. They also play certain roles in wood processing and related applications [4, 5]. Shebani et al. [6] reported that the thermal stability of wood polymer composites made with four extractive-free wood species is higher than the untreated controls. This was because the higher extractive contents associated with lower crystallinity and lower cellulose crystallite size could accelerate the degradation process [7]. While wood extractives may include an array of compounds (e.g., aliphatic, terpenoid, and phenolic) in nature, the detailed characterization of their molecular compositions by advanced instrumental techniques are very limited [8].

Wood extractives can also change the wettability and the curing properties of wood adhesives, thus affecting the gluing bond strength and performance [5, 9, 10]. Maple and oak are two wood substrates frequently used in wood adhesive studies [11, 12, 13, 14, 15]. Increased knowledge on the water extractives from the two types of wood would be helpful in better understanding, and thus improving the strategies, of wood-adhesive bonding. However, there is limited documentation of compounds or extractives from maple and oak wood types. Therefore, the objective of this research was to identify and characterize the chemical composition of the water soluble materials (i.e., extractives) from maple and oak wood veneers. The long-term goal is to apply the knowledge of wood extractives to develop better strategies for improving the adhesive-wood bonding interactions by changing surface polarity, wettability and permeability of the bonding interface [16]. To do so, in this study, chemical compounds in maple and oak strips were extracted with water. The chemical composition of

the water extractives was compared and characterized by ultraviolet/visible (UV/vis) spectroscopy and ultrahigh resolution Fourier transform ion cyclotron resonance mass spectrometry (FT-ICR-MS) using both negative and positive electrospray ionization (ESI) modes.

2. Materials and Methods

2.1. Wood materials

Maple and white oak veneers (1.59 mm thick) were purchased from Certainly Wood, Inc. (East Aurora, NY, USA). The wood veneers were cut into strips (12 for each wood type) 25.4 mm wide by 88.9 mm long, with the wood grain parallel to the long side, and stored in sealed plastic bags until used. The maple density was 0.79 g cm^{-3}, and the moisture content under the conditioning environment was 9.16% on a dry basis. The oak density was 0.77 g cm^{-3}, with the moisture content under the conditioning environment being 9.29% on a dry basis [17, 18].

2.2. Sample extraction

The wood strips used in extractions were equilibrated in a humidity controller with 50% relative humidity (RH) for at least one week at 22 °C. Each set of 12 wood strips was soaked in distilled water (800 mL) for 2 days at 22 °C with occasional shaking. After removal of the soaked wood strips, 15 ml of the soaking water was retained, and the remaining was dried in a vacuum oven at 60 °C. The soaked wood strips were dried at 22 °C in the humidity controller with 50% RH (make, model, city of drier), and the weight loss was used to calculate the extraction efficiency (yield) on a dry weight basis. Triplicate extractions were conducted for each type of wood. The white oak extract was a dark brown/black solid, while the maple extract was an amber brown solid.

2.3. Ultraviolet-visible (UV–vis) spectral analysis

The UV-vis spectra of diluted water extractives of oak and maple using 1.5-ml quartz cuvettes were recorded at the wavelengths of 200-700 nm with an Evolution 60S UV-visible spectrophotometer (Thermo Scientific, Madison, WI). The scan speed mode was set at medium level with the interval of 1 nm. Standard 10-mm path length quartz cells were used for measurement. To obtain the absorbance in the measurable range, the spectra were recorded with the undiluted samples, as well as after diluting by factors of 10-100 with water. UV-vis spectral features of E2/E3 and E4/E6 were calculated from the ratios of the absorbance at 250 and 365 nm and at 400 and 600 nm, respectively [19].

2.4. ESI FT-ICR mass spectrometry

The vacuum-dried wood extractives were dissolved at approximately 1 mg mL^{-1} in ultrahigh quality (UHQ) H_2O at pH 8 adjusted with NH_4OH. All solids appeared to dissolve completely, giving an amber brown solution for the oak sample and light brown solution for the maple sample. Each sample was then diluted by a factor of 4 to give a final sample composition of 1:1 H_2O:MeOH (methanol, LC-MS grade, Fisher Scientific).

Samples were analyzed in both negative and positive ESI modes. The two diluted samples were continuously infused into an Apollo II ESI ion source of a Bruker Daltonics 12 Tesla Apex Qe FTICR-MS, introduced by a syringe pump operating at 120 μL hr^{-1} with the same parameter set-up as reported previously [20]. ESI voltages were optimized for each sample to maintain consistent and stable ion currents. In order to balance peak resolving powers with signal to noise (S/N) ratios, ions were accumulated for 1.0 sec in a hexapole before being transferred to the ICR cell, where 300 transients, collected with a 4 MWord time domain, were co-added, giving about a 30 min total run time. The summed FID signal was zero-filled once and Sine-Bell apodized prior to fast Fourier transformation and magnitude calculation using the Bruker Daltonics Data Analysis software.

Prior to mass spectral data analysis in both positive and negative ion modes, samples were externally calibrated with a polyethylene glycol (PEG) standard and internally calibrated with fatty acids, dicarboxylic acids, and other naturally present ions within the sample [21]. Formula assignments were based on a list of conservative rules that ensure the formulas are chemically possible in nature and would ionize in either positive or negative ion mode [22, 23]. Empirical formulas were generated by a molecular formula calculator using C, H, O, N, and S ($C_{5-50}H_{5-100}O_{0-30}N_{0-4}S_{0-2}$) within 1 ppm mass error. For positive ion mode, 1 Na atom was allowed per formula. Only m/z values with an S/N ratio above 3 were inserted into the molecular formula calculator. The assigned formulas, in the vast majority of cases, agreed within an error value of $\leq$0.5 ppm of the calculated exact mass of the assigned formulas.

2.5. Data collection and analysis

The yield and UV-vis parameters of wood extractives were analyzed by Proc Means of the Statistical Analysis System (SAS Version 9.2; SAS institute, Cary, NC) to generate means and associated standard errors. The UV-vis spectra, as well as the negative and positive ion ESI FT-ICR mass spectra, of the water extractives of maple and oak were obtained and graphically plotted to visualize their characteristics. The biomolecular compound classes of maple and oak extractives were categorized and plotted using two-dimensional van Krevelen diagrams. The total number of formulas and selected molecular-level parameters were computed and tabulated for treatment combinations. Similarly, the diversity (number and percentage of formulas), as well as their relative frequency or abundance, of biomolecular compound classes were also computed.

3. Results and Discussion

3.1. Extraction yield

The yield of water extraction was 3.14% and 2.93%, for maple and oak, respectively, on a dry mass basis (Table 1). These values were in the range of extraction efficiency of various wood materials. Generally, wood extractives account for 2-5% of wood content, even though higher yields could be reached in certain types of wood or by different extractants [8, 24]. For example, Malik and Santoso [4] reported extraction efficiencies in the range of 0.7-6.7% for oily keruing wood samples using solutions of water and ethanol in various proportions. Malik et al. [1] reported that the extraction yield of merbau extractives were 12.45%, 12.56%, and 1.34% when 80% ethanol, 60% ethyl acetate, and hot water were used, respectively. The organic solvents increase the extractive efficiency due to the fact that their polar and non-polar functional groups dissolve more complicated compounds, such as tannins, resins, wax, and gum. The solvent choice should depend on the targeted extracted compounds and/or the purpose of the extraction. From a general environmental point of view, water is better than organic solvents, because it is relatively cheap, nontoxic, inflammable, and recyclable [1]. As the primary purpose of this work was characterizing the water-soluble materials in wood veneers, water was the best choice.

3.2. The UV-Vis spectral features

The triplicate samples of each type of wood extractive showed almost identical spectral features with minor strength differences (Fig. 1). The UV-vis spectral features of the oak extractives have monotonically-decreasing curves with increasing wavelength and two absorbance shoulders around 225 and 279 nm, except for a peak near 210 nm. This featureless characteristic of the UV-vis spectra is common for natural organic matter, which indicates that there were many different chromophores in this complex sample [19]. The abundant

chromophores could be aromatic and/or phenolic compounds with conjugated C=C and C=O double bonds, which have strong absorbances in the range of 200 nm to 300 nm, as described in earlier studies of wood extractives [25] and other plant extracts [26]. In the spectra of the maple extracts, the absorbance shoulder at 279 nm was a distinct absorbance peak. Therefore, in the maple extractives, some chromophores were apparently more abundant than in oak extractives. Malik et al. [1] attributed a strong UV-peak at the similar 279 nm in their merbau extractives to the phenolic compound resorcinol, by comparison to the UV-vis spectrum of the model compound.

Quantitatively, the value of E2/E3 was about 17 for the oak extractives per the measurements of A_{250} and A_{365} with the 1/100x and 1/20x diluted samples (Table 1). The value was near 6 for the maple extractives per the measurements with the 1/50x and 1/10x diluted samples. The visible absorbance, especially at 600 nm, was quite low, and as such, the undiluted samples were used to obtain the E4/E6 ratios. These data show that both of the E2/E3 and E4/E6 parameters were higher in the oak extractives than in the maple extractives. These two UV-vis ratios are widely used for the characterization of labile organic matter from various sources of soil and environmental samples [27, 28, 29, 30]. The E4/E6 value was also used as a colloidal parameter of the water-soluble materials in the composting of forestry waste (oak biomass) [31]. Higher E2/E3 values may reflect lower average molecular mass components. Higher E4/E6 values may be contributed by both lower average molecular mass components and less aromatic structures. Waldrip et al. [28] reported an E2/E3 value of about 7.2 for surface beef manure, but around 3.5 in its sediment samples. The authors attributed their observations that the surface manure was more recently excreted materials with lower molecular mass (i.e., no humification). In humic acid samples, He et al. [32] observed that E4/E6 values were 3.6 and 15, respectively, for the acid's high (> 3 KD) and low (<3 KD) molecular mass fractions. Based on these earlier observations, the two sets of E2/E3 and E4/E6 values recorded in this study

imply that the maple extractives possessed higher molecular mass and more aromatic components than the oak extractives.

3.3. ESI FT-ICR mass spectral features

The broadband ESI FT-ICR mass spectra of the two extractives are shown in Fig. 2. For both samples, peaks were mainly detected at m/z 250-800. However, apparent differences were observed in the spectral features between the two samples, and between the different ionization modes of the same sample. For both ESI modes, the maple sample showed strong peaks in the range of m/z 320-380, with modestly strong peaks between m/z 500-700 using negative ion mode. In contrast, strong peaks were detected in the wider range of m/z 420-620 in the oak extractives with negative ion mode and a more narrow range of m/z 400-480 with positive ion mode. The ultrahigh resolving powers of FT-ICR-MS allowed for the separation of m/z values to a mass accuracy of less than 1 ppm. Thus, numerous peaks could be detected at each nominal mass within an error value of less than 0.5 ppm compared to the calculated exact mass of the assigned formulas (insets of Fig. 2). In total, negative ion mode analysis allowed for the assignment of 2781 formulas in the maple extractives and 2256 formulas in the oak extractives (Table 2). Positive ion mode detected fewer peaks (and thus less formulas), with 924 and 1009 formulas for the maple and oak samples, respectively. The difference between the two ion modes is due to the fact that positive ESI produces mostly proton adducts or cation adducts, i.e., $[M + H]^+$ or $[M + Na]^+$; and negative ESI produces mostly deprotonated compounds, i.e., $[M - H]^-$ [33]. As a result, positive ESI could represent more of those molecules with high proton affinities, and negative ESI enhances ion signals for acidic compounds. It should be noted that low molecular weight compounds, such as resorcinol ($C_6H_6O_2$, 110.112 Da) featured in the UV-vis spectra (Fig. 1), are not efficiently detected by FT-ICR0MS, and thus, the bulk elemental compositions may differ [20, 34]. Other hyphened MS techniques could be applied to detect the smaller ions, such as GC-MS and analytical pyrolysis-MS [35, 36].

The average m/z for the water extractives of maple were 546 and 477 for negative and positive ion modes, respectively (Table 2). For the water extractives of oak in negative and positive ion mode, the average m/z values were 534 and 457, respectively, which are slightly lower than the values for maple, which is consistent with the absorbance ratio indications previously described from the UV-vis spectra. The average number of carbons and O/C ratios were similar between the two samples for each ion mode. H/C ratios are inversely proportional to DBE values, as high H/C ratios indicate a more aliphatic character and high DBE ratios indicate a more aromatic character. For both ion modes, the maple sample was less aromatic (i.e., had higher H/C and lower DBE) than the oak sample. These observations are consistent with oak having higher overall UV absorbances (Fig. 1), but inconsistent with the E4/E6 ratio that suggested that oak was less aromatic than the maple. This inconsistency likely points towards a fraction of the oak water extractive that is aromatic but not ionized by ESI in either ion mode, which suggests a pure hydrocarbon that would be ionized by atmospheric pressure photoionization (APPI). These data are in the range of other organic materials, such as bio-oil products, water extracts of plant, and organic humic acid fractions (Table 1). The average O/C ratios and DBE values of the two wood extractives are higher than other organic samples, but within the typical range for dissolved organic matter extracted from aquatic sources.

3.4. van Krevelen (V-K) analysis

Table 3 summarizes the distribution of the formulas (by both number and magnitude) based on the heteroatom content (CHO(Na), CHON (Na), and CHOS (Na), where Na was only included for positive ion mode data). For both extractives, more than 90% of the formulas fall in the CHO and CHON categories. Using negative ion mode, 6% of the formulas (accounting for 7% of the total spectral magnitude) were CHOS and were assigned in the maple extractives, but even less (2% of formulas accounting for 1% of the total spectral magnitude) were in the oak extractives.

To better visualize and compare the chemical compositions of the maple and oak water extractives, V-K diagrams were plotted and formulas were grouped into 7 biomolecular compound classes (Figs. 3 and 4). Nearly all formulas aligned within a compound classes, leaving only 2-3% of the formulas (accounting for 1-3% of the total spectral magnitude, Table 4) falling outside one of these ranges. While there are less formulas in the positive ion mode data, the patterns in the distribution of compound categories within the V-K diagrams between the two ion modes looks quite similar. The patterns of the V-K diagrams of the two extractives were similar to that of steam-treated pine biomass samples dominated by carbohydrates and lignins, although there were only 10 data points obtained from bulk elemental analysis [37]. While lignins are generally considered to be essentially hydrophobic (or lipophilic) [37], the lignin-like formulas in the water extractives may be devoted to the hydrophilic precursors and/or degradation products of lignins [38, 39]. The patterns of the V-K diagrams of the two extractives were also similar to that of the V-K diagram of short-rotation willow fast pyrolysis oil observed with negative ion mode FT-ICR MS, except more lipids, as expected, were observed in the bio-oil [24].

In general, the O/C averages are fairly similar between the extractives of maple and oak. However, maple sample possessed a higher average H/C (and thus lower DBE). As such, there are more aliphatic formulas in the maple samples, and more aromatic formulas in the oak samples. For both samples, most of the formulas contain CHO-only, but they do both contain some CHON and CHOS formulas. The V-K diagrams visually show that most of the formulas fall into the lignin-like (approximate boundaries of O/C 0.1-0.6 and H/C 0.5-1.7) and carbohydrate-like (approximate boundaries of O/C 0.6-1.2 and H/C 1.5-2.2) regions, with some contributions in the tannin-like (approximate boundaries of O/C 0.6-1.2 and H/C 0.5-1.5) and lipid-like (approximate boundaries of O/C 0.0-0.2 and H/C 1.7-2.2) regions. Quantitatively, lignin-like components are the most diversified, accounting for 53-75% of the formulas (and

35-81% of the total spectral magnitude, Table 4). Carbohydrate- and tannin-like compounds exist in moderate abundance and diversity, accounting for about 10-24% of detected formulas and 8-39% of the abundance. Peptide- and lipid-like are also present in both extractives but in small amounts (<3%). Positive ion mode did detect more peptide-like components, as peptides are N-containing compounds that are typically ionized more efficiently in positive mode. Condensed aromatics and unsaturated hydrocarbons were essentially negligible.

3.5. Characteristics of major compounds

Although thousands of formulas were identified in the wood extractives by FT-ICR-MS, the top 25 formulas detected in highest magnitude accounted for the much (nearly 50%) of the total spectral magnitude of all formulas in negative ion mode (Tables 5 and 6). Furthermore, the abundance of the top 5 formulas accounted for 30.1% and 49.3% of total magnitude in the maple extractives, and 32.2% and 19.0% in the oak extractives, using negative and positive ion mode, respectively. With the exception of one formula, all of the top 25 formulas belong to the lignin-like, carbohydrate-like, or tannin-like classes. The one exception is the peak at m/z 329.2333 with an abundance of 0.523%, assigned to $C_{18}H_{33}O_5$, which could be 9,12,13-trihydroxyoctadecenoate or any of its structural isomers [40]. There are five formulas that appeared twice in the top 25 peaks of the maple and oak extractives. Three formulas ($C_{22}H_{37}O_{19}$, $C_{29}H_{31}O_{12}$, and $C_{27}H_{31}O_{10}$) were detected in negative ion mode of both the maple and oak extractives, and one formula ($C_{22}H_{26}O_9Na$) appeared in positive ion mode of both extractives. These results implied that the four formulas should be major components in both wood samples. One formula ($C_{22}H_{27}O_8$) appeared in both negative and positive ion mode spectra of the oak sample, probably representing the zwitterion properties of the compound. While two S-containing lignins and one tannin were in the top 25 peaks of the maple extractives, no S-containing compound was in the top 25 peaks of the oak extractives. Among the three S-containing formulas, $C_{22}H_{25}O_{11}S$ has been reported as a fragment of paeoniflorin sulfonate

($C_{23}H_{27}O_{13}S$), a newly-generated marker due to sulfur-fumigation of Moutan Cortex (a root bark) [41]. While there is no information on the history of the two wood samples we studied, it would be of interest to investigate further the origin of these S-containing compounds in the maple sample.

We further explored possible identities of the top 5 peaks of each spectrum. The highest peak (13.6% of the total spectral magnitude) using negative ion mode for the maple extractives was at m/z 341.1087. Its formula was assigned to $C_{12}H_{21}O_{11}$, which could be dihexoside. Its abundance could be due to the presence of various dihexoside derivatives found in nature, such as pine cones [42]. The second highest peak (7.2%) at m/z 683.2246 seemed to be a dimer of dihexoside, having a formula of $C_{24}H_{43}O_{22}$. The third abundant peak was lignin-like but having 4 N atoms and 14 DBEs with the formula $C_{24}H_{25}O_{10}N_4$, which could not be found in the literature. The fourth abundant formula ($C_{31}H_{37}O_{11}$) is related to the products of natural hypolignification [43]. The fifth formula ($C_{18}H_{31}O_{16}$) could be a 6-kestose monohydrate [44].

The highest peak (30.7% of the total spectral magnitude) of the maple extractives in positive ion mode is at m/z 381.0792, assigned to $C_{15}H_{18}O_{10}Na$. This chemical is a glucuronoconjugate, which has not been well documented but found in neuroblastoma patients [45]. The second highest peak (9.5%) at m/z 365.1053 ($C_{12}H_{22}O_{11}Na$) could be a 6,6'-linked disaccharide, such as 6-O-(6-Deoxy-D-allos-6-yl)-D-allose and 6-O-(6-Deoxy-α-D-mannopyranos-6-yl)-α-D-mannopyranose, previously reported in their relevance to the root of the thorny palm *Acrocomia mexicana* [46]. The formula ($C_{18}H_{18}O_8Na$) and exact mass (385.0894) of the third peak are equal to the values of lepraric acid in metabolite profiling of lichens by an LC–MS method [47]. The fourth and fifth peaks could be classified as artoheterone ($C_{17}H_{16}O_7Na$) [48] and sucrose ($C_{12}H_{26}O_{11}N$, $[M+NH4]^+$) [49], respectively.

In the oak extractives, the highest peak (14.2% of the total spectral magnitude) using negative ion mode was at m/z 419.1708 with a formula of $C_{22}H_{27}O_8$. This peak could be assigned to lyoniresinol, which has been documented in oak extractives and maple sap [50, 51]. As a major component of oak, it is also found in the positive ion mode spectrum of the oak extractives with an abundance of 1.8%, which is still in the top 25. This chemical is also present in the maple extractives, but with a much lower magnitude (0.03% and 0.02% using negative and positive ion modes, respectively). The second abundant peak ($C_{22}H_{31}O_{12}$, 6.7%) could be assigned to caffeoyl hexose-deoxyhexoside, which is found in fruit tree biomass, such as avocado (*Persea americana*) [52]. The formula ($C_{22}H_{37}O_{19}$) of the third peak (5.7%) is also in the top 25 formulas of the maple extractive with a relative abundance of 1.1%. It fits the molecular formulas for deaminoneuraminic acid-α-2,6-lactoside-β-OCH_3 and deaminoneuraminic acid-α-2,3-lactoside-β-OCH_3 [53]. The fourth peak with the formula of $C_{28}H_{37}O_{13}$ could be a tinosposinenside, as detected in the stems of *Tinospora sinensis* plants [54]. The fifth peak at m/z 551.2134 still possessed a relatively high magnitude (1.4%), but no published information on its identity ($C_{21}H_{37}O_{12}$) was available.

The relative abundance of the first peak in the oak extractives using positive ion mode was 9.8%, which is lower than the relative abundance of the first peak of other spectra. However, the abundance was still much higher than the next 4 peaks in the top 5 that were all approximately 2.0% (Table 6). The first peak could be assigned to the formula $C_{25}H_{24}O_7Na$ with a structural possibility of tert-butyl 4-hydroxy-6'-methoxy-2'-methyl-2-oxo-2H,4'H-[3,4'-bichromene]-3'-carboxylate [55]. The formula of the second peak is similar to the first one but with one more DBE ($C_{25}H_{22}O_7Na$), which could be artobiloxanthone or cycloartobiloxanthone found in evergreen trees *Artocarpus rigida* Blume (Moraceae, mulberry family) [56]. The third one ($C_{22}H_{23}O_7$) could be 6-Oxo-6-{4-[(4-propoxybenzoyl)oxy]phenoxy}hexanoate or yatein, a lignin isolated from evergreen trees and

other sources [57]. The fourth formula ($C_{22}H_{28}O_8Na$) could be a eupachinisin product that has been isolated from a whole plant extract of *Eupatorium chinense* [58]. There was no match found for the fifth formula ($C_{19}H_{26}O_{12}N$) based on literature searches.

4. Conclusions

This work showed that about 3% of chemical components in maple and oak were extractable by water. UV-vis spectral data indicated that the maple extractives possessed higher molecular mass and more aromatic components than the oak extractives. UV-vis spectra indicated the presence of the phenolic compound resorcinol ($C_6H_6O_2$, 110.112 Da) in the maple extractives. ESI FT-ICR-MS analysis provided more molecular-level information on the composition of the wood extractives, which have a molecular weight range of 200-800 Da. For both extractives, more than 90% of the formulas fell into the CHO and CHON heteroatom categories. With negative ion mode, 6% of the formulas, which account for 7% of the total spectral magnitude, were CHOS formulas detected in the maple extractives, but only 2% of the formulas (1% of the total spectral magnitude) were in the oak extractives. Lignin-, carbohydrate-, and tannin-like compounds were the three major categories of biomolecules detected. In this research, negative ion ESI allowed for the detection of >2500 formulas, while positive ion mode allowed for the detection of about 1000 formulas. Moreover, the top 25 most abundant peaks (i.e., formulas) accounted for 47.1% and 63.8% of the total spectral magnitude of all formulas in the maple extractives using negative and positive ion mode, respectively. About 45.5% and 33.5% of the total spectral magnitude was due to the 25 most abundant peaks in the oak sample using negative and positive ion mode, respectively. The profiles of the top 25 formulas differed between the two wood samples, although 4 formulas appeared in the spectra of both samples. Among the 20 formulas of the top 5 from the 4 spectra, 17 could be connected to specific bioactive chemical compounds related to tree and other plant biomass, based on the literature comparisons. Thus, data and observations in this

research increased the knowledge of wood chemistry for exploration of bioactive chemicals in wood extractives, as well as provided some information for further applications of FT-ICR-MS for chemical markers useful in profiling and identification of wood types and sources [36, 59].

Acknowledgements

Mention of trade names or commercial products in this publication is solely for the purpose of providing specific information and does not imply recommendation or endorsement by the U.S. Department of Agriculture. USDA is an equal opportunity provider and employer.

References

1. Malik J, Santoso A, Mulyana Y, Ozarska B. Characterization of Merbau extractives as a potential wood-impregnating material. BioResources. 2016;11:7737-53.
2. Roffael E. Significance of wood extractives for wood bonding. Appl Microbiol Biotechnol. 2016;100:1589-96.
3. Tittikpina NK, Nana F, Fontanay S, Philippot S, Batawila K, Akpagana K. Antibacterial activity and cytotoxicity of pterocarpus erinaceus poir extracts, fractions and isolated compounds. J Ethnopharmacol. 2018;212:200-7.
4. Malik J, Santoso A. Effect of extractive-dissolving treatment on the characteristics of laminated wood assembled from oily keruing wood. J Agri Sci Technol B. 2011;1:1191-6.
5. Bockel S, Mayer I, Konnerth J, Niemz P, Swaboda C, Beyer M, Harling S, Weiland G, Bieri N, Pichelin F. Influence of wood extractives on two-component polyurethane adhesive for structural hardwood bonding. J Adhes. 2018;94:829-45.
6. Shebani A, Van Reenen A, Meincken M. The effect of wood extractives on the thermal stability of different wood-LLDPE composites. Thermochim Acta. 2009;481:52-6.
7. Poletto M, Zattera AJ, Forte MM, Santana RM. Thermal decomposition of wood: Influence of wood components and cellulose crystallite size. Bioresour Technol. 2012;109:148-53.
8. Yin X, Huang A, Zhang S, Liu R, Ma F. Identification of three dalbergia species based on differences in extractive components. Molecules. 2018;23:2163.
9. Hse C-Y, Kuo M-L. Influence of extractives on wood gluing and finishing-a review. Forest Prod J. 1988;38:52-6.
10. Tohmura S-i. Acceleration of the cure of phenolic resin adhesives VII: Influence of extractives of merbau wood on bonding. J Wood Sci. 1998;44:211-6.
11. Cheng HN, Wyckoff W, Dowd MK, He Z. Evaluation of adhesion properties of blends of cottonseed protein and anionic water-soluble polymers. J Adhes Sci Technol. 2019 33:66-78.

12. He Z, Chapital DC, Cheng HN, Olanya OM. Adhesive properties of water-washed cottonseed meal on four types of wood. J Adhes Sci Technol. 2016;30:2109-19.
13. He Z, Cheng HN, Klasson KT, Olanya OM, Uknalis J. Effects of particle size on the morphology and water- and thermo-resistance of washed cottonseed meal–based wood adhesives. Polymers. 2017;9:675. http://dx.doi.org/10.3390/polym9120675.
14. Liu M, Wang Y, Wu Y, He Z, Wan H. "Greener" adhesives composed of urea-formaldehyde resin and cottonseed meal for wood-based composites. J Cleaner Prod. 2018;187:361-71.
15. Pradyawong S, Li J, He Z, Sun XS, Wang D, Cheng HN, Klasson KT. Blending cottonseed meal products with different protein contents for cost-effective wood adhesive performances. Ind Crop Prod. 2018;126:31-7.
16. Bockel S, Mayer I, Konnerth J, Harling S, Niemz P, Swaboda C, Beyer M, Bieri N, Weiland G, Pichelin F. The role of wood extractives in structural hardwood bonding and their influence on different adhesive systems. Int J Adhes Adhes. 2019;91:43-53.
17. Sánchez ML, Morales LY, Caicedo JD. Physical and mechanical properties of agglomerated panels made from bamboo fiber and vegetable resin. Construction and Building Materials. 2017;156:330-9.
18. Nguyen DM, Grillet A-C, Diep TMH, Bui QB, Woloszyn M. Influence of thermo-pressing conditions on insulation materials from bamboo fibers and proteins based bone glue. Ind Crop Prod. 2018;111:834-45.
19. Zhang M, He Z. Characteristics of dissolved organic carbon revealed by ultraviolet–visible absorbance and fluorescence spectroscopy: the current status and future exploration. In: He Z, Wu F, editors. Labile Organic Matter - Chemical Compositions, Function, and Significance in Soil and the Environment SSSA Special Publication 62. Madison, WI: Soil Sci. Soc. Am.; 2015. p. 1-22.
20. He Z, Guo M, Sleighter RL, Zhang H, Fortier CA, Hatcher PG. Characterization of defatted cottonseed meal-derived pyrolysis bio-oil by ultrahigh resolution electrospray ionization Fourier transform ion cyclotron resonance mass spectrometry. J Anal Appl Pyrol. 2018;136:96-106.
21. Sleighter RL, Hatcher PG. Molecular characterization of dissolved organic matter (DOM) along a river to ocean transect of the lower Chesapeake Bay by ultrahigh resolution electrospray ionization Fourier transform ion cyclotron resonance mass spectrometry. Marine Chem. 2008;110:140-52.
22. Stubbins A, Hood E, Raymond PA, Aiken GR, Sleighter RL, Hernes PJ, Butman D, Hatcher PG, Striegl RG, Schuster P. Anthropogenic aerosols as a source of ancient dissolved organic matter in glaciers. Nature Geoscience. 2012;5:198-201.
23. Hockaday WC, Grannas AM, Kim S, Hatcher PG. Direct molecular evidence for the degradation and mobility of black carbon in soils from ultrahigh-resolution mass spectral analysis of dissolved organic matter from a fire-impacted forest soil. Org Geochem. 2006;37:501-10.
24. Miettinen I, Kuittinen S, Paasikallio V, Makinen M, Pappinen A, Janis J. Characterization of fast pyrolysis oil from short-rotation willow by high-resolution Fourier transform ion cyclotron resonance mass spectrometry. Fuel. 2017;207:189-97.
25. Segoloni E, Di Maria F. UV–VIS spectral and GC–MS characterization of Handroanthus serratifolius (Vahl.) Grose (aka Tabebuia serratifolia (Vahl.) Nichols/Lapacho) heartwood main extractives: a comparison of protocols aimed at a practical evaluation of Lapachol and Dehydro-α-Lapachone content. Eur J Wood Wood Prod. 2018;76:1547-61.
26. He Z, Mao J, Honeycutt CW, Ohno T, Hunt JF, Cade-Menun BJ. Characterization of plant-derived water extractable organic matter by multiple spectroscopic techniques. Biol Fertil Soils. 2009;45:609-16.

27. Zhao A, Zhang M, He Z. Spectroscopic characteristics and biodegradability of cold and hot water extractable soil organic matter under different land uses in subarctic Alaska. Commun Soil Sci Plant Anal. 2013;44:3030-48.
28. Waldrip HM, He Z, Todd RW, Hunt JF, Rhoades MB, Cole NA. Characterization of organic matter in beef feedyard manure by ultraviolet-visible and Fourier transform infrared spectroscopies. J Environ Qual. 2014;43:690-700.
29. Cuss CW, Gueguen C. Characterizing the labile fraction of dissolved organic matter in leaf leachates: methods, indicators, structure, and complexity. In: He Z, Wu F, editors. Labile Organic Matter-Chemical Compositions, Function, and Significance in Soil and the Environment. Madison, WI: Soil Sci. Soc. Am.; 2015. p. 237-74.
30. He Z, Zhang M, Zhao A, Olanya OM, Larkin RP, Honeycutt CW. Quantity and nature of water-extractable organic matter from sandy loam soils with potato cropping management. Agric Environ Lett. 2016;1:160023 (6 pages). doi:10.2134/ael2016.06.0023.
31. Martínez-Iñigo M-J, Almendros G. Kinetic study of the composting of evergreen oak forestry waste. Waste manag Res. 1994;12:305-14.
32. He Z, Ohno T, Cade-Menun BJ, Erich MS, Honeycutt CW. Spectral and chemical characterization of phosphates associated with humic substances. Soil Sci Soc Am J. 2006;70:1741-51.
33. Cole DP, Smith EA, Dalluge D, Wilson DM, Heaton EA, Brown RC, Lee YJ. Molecular characterization of nitrogen-containing species in switchgrass bio-oils at various harvest times. Fuel. 2013;111:718-26.
34. Kekalainen T, Venalainen T, Janis J. Characterization of birch wood pyrolysis oils by ultrahigh-resolution fourier transform ion cyclotron resonance mass spectrometry: insights into thermochemical conversion. Energy Fuels. 2014;28:4596-602.
35. Wang JJ, Dodla SK, He Z. Application of analytical pyrolysis-mass spectrometry in characterization of animal manure. In: He Z, editor. Environmental Chemistry of Animal Manure. NY: Nova Science Publishers; 2011. p. 3-24.
36. Bisht SS, Na MK, Ezhumalaia R, Kumarb R. Spectroscopic techniques and their application in metabolic profiling of wood and wood based material: A mini-review. Appl Sci Adv Mater Int. 2015;1:79-84.
37. Negro M, Manzanares P, Oliva J, Ballesteros I, Ballesteros M. Changes in various physical/chemical parameters of Pinus pinaster wood after steam explosion pretreatment. Biomass Bioenerg. 2003;25:301-8.
38. D'Auria M, Emanuele L, Racioppi R. A FT-ICR MS analysis of lignin. Nat Prod Res. 2012;26:1368-74.
39. Kujawinski EB, Freitas MA, Zang X, Hatcher PG, Green-Church KB, Jones RB. The application of electrospray ionization mass spectrometry (ESI MS) to the structural characterization of natural organic matter. Organic Geochem. 2002;33:171-80.
40. Hamberg M. Regio- and stereochemical analysis of trihydroxyoctadecenoic acids derived from linoleic acid 9- and 13- hydroperoxides. Lipids. 1991;26:407-15.
41. Li XY, Duan SM, Liu HH, Xu JD, Kong M, Liu HQ, Li SL. Sulfur-containing derivatives as characteristic chemical markers in control of sulfur-fumigated moutan cortex. Yao Xue Xue Bao (Acta pharmaceutica Sinica). 2016;51:972-8.
42. Wang L, Li X, Wang H. Physicochemical properties, bioaccessibility and antioxidant activity of the polyphenols from pine cones of Pinus koraiensis. Int J Biol Macromol. 2019;126:385-91.
43. Huis R, Morreel K, Fliniaux O, Lucau-Danila A, Fénart S, Grec S, Neutelings G, Chabbert B, Mesnard F, Boerjan W. Natural hypolignification is associated with extensive oligolignol accumulation in flax stems. Plant Physiol. 2012;158:1893-915.

44. Ferretti V, Bertolasi V, Gilli G, Accorsi C. Structure of 6-kestose monohydrate, C18H31O16. H2O. Acta Crystallograph Section C: Crystal Struct Commun. 1984;40:531-5.
45. Scapolla C, Cangemi G, Barco S, Barbagallo L, Bugnone D, Maffia A, Melioli G, Profumo A, Benatti U, Damonte G. Identification and structural characterization by LC-ESI- IONTRAP and LC- ESI- TOF of some metabolic conjugation products of homovanillic acid in urine of neuroblastoma patients. J Mass Spectrom. 2012;47:816-24.
46. Haines AH. Synthesis of 6,6′-ether linked disaccharides from D-allose, D-galactose, D-glucose and D-mannose; evidence on the structure of coyolosa. Org Biomol Chen. 2004;2:2352-8.
47. Parrot D, Peresse T, Hitti E, Carrie D, Grube M, Tomasia S. Qualitative and spatial metabolite profiling of Lichens by a LC–MS approach combined with optimised extraction. Phytochem Anal. 2015;26:23-33.
48. Ren G, Peng J, Liu A, Liang J, Yuan W, Wang H, He J. Structure elucidation and NMR assignments of two new flavanones from the roots of Artocarpus heterophyllus. Magnet Resonan Chem. 2015;53:872-4.
49. Xue S, Wang L, Chen S, Cheng Y. Simultaneous analysis of saccharides between fresh and processed radix rehmanniae by HPLC and UHPLC-LTQ-Orbitrap-MS with multivariate statistical analysis. Molecules. 2018;23:541.
50. Winstel D, Marchal A. Lignans in Spirits: Chemical Diversity, Quantification, and Sensory Impact of (±)-Lyoniresinol. Molecules. 2019;24:117.
51. Liu Y, Rose KN, DaSilva NA, Johnson SL, Seeram NP. Isolation, Identification, and Biological Evaluation of Phenolic Compounds from a Traditional North American Confectionery, Maple Sugar. J Agric Food Chem. 2017;65:4289-95.
52. Castro-López C, Bautista-Hernández I, González-Hernández M, Martínez-Ávila G, Rojas R, Gutiérrez-Díez A, Medina-Herrera N, Aguirre-Arzola V. Polyphenolic profile and antioxidant activity of leaf purified hydroalcoholic extracts from seven Mexican Persea americana cultivars. Molecules. 2019;24:173.
53. Wei M. Transforming Dihydroxyacetone Phosphate-Dependent Aldolases Mediated Aldol Reactions From Flask Reaction Into Cell-Based Synthesis & Studying The Mechanism Of Chemical Desialylation In The Life Processes." Dissertation, Georgia State University, ps://scholarworks.gsu.edu/chemistry_diss/121 2016.
54. Xu L-L, Guo F-X, Chi S-S, Wang Z-J, Jiang Y-Y, Liu B, Zhang J-Y. Rapid screening and identification of diterpenoids in Tinospora sinensis based on high-performance liquid chromatography coupled with linear ion trap-Orbitrap mass spectrometry. Molecules. 2017;22:912.
55. Rao LC, Kumar NS, Dileepkumar V, Murthy U, Meshram H. “On water” synthesis of highly functionalized 4 H-chromenes via carbon–carbon bond formation under microwave irradiation and their antibacterial properties. RSC Advances. 2015;5:28958-64.
56. Ren Y, Kardono LB, Riswan S, Chai H, Farnsworth NR, Soejarto DD, Carcache de Blanco EJ, Kinghorn AD. Cytotoxic and NF-κB inhibitory constituents of Artocarpus rigida. J Nat Prod. 2010;73:949-55.
57. Miyata M, Itoh K, Tachibana S. Extractives of Juniperus chinensis L. I: Isolation of podophyllotoxin and yatein from the leaves of J. chinensis. J Wood Sci. 1998;44:397-400.
58. Yu X, Zhang Q, Tian L, Guo Z, Liu C, Chen J, Ebrahim W, Liu Z, Proksch P, Zou K. Germacrane-type sesquiterpenoids with antiproliferative activities from eupatorium chinense. J Nat Prod. 2017;81:85-91.
59. Kite GC, Green PW, Veitch NC, Groves MC, Gasson PE, Simmonds MS. Dalnigrin, a neoflavonoid marker for the identification of Brazilian rosewood (Dalbergia nigra) in CITES enforcement. Phytochem. 2010;71:1122-31.

60. Ohno T, He Z, Sleighter RL, Honeycutt CW, Hatcher PG. Ultrahigh resolution mass spectrometry and indicator species analysis to identify marker components of soil- and plant biomass-derived organic matter fractions. Environ Sci Technol. 2010;44:8594-600.

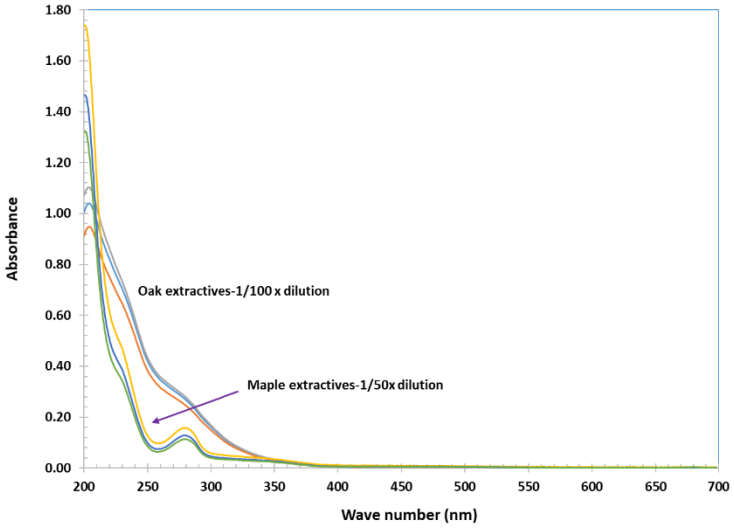

Fig. 1. UV-vis spectra of triplicate water extractives of oak and maple.

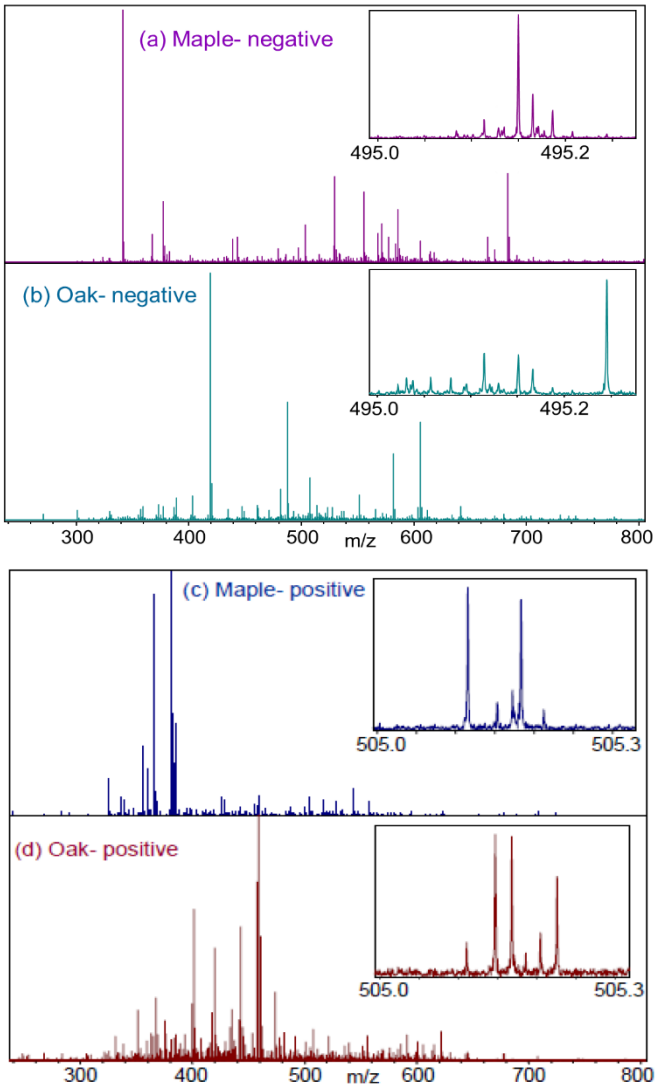

Fig. 2. Negative and positive ion ESI FT-ICR mass spectra of water extractives of oak and maple wood.

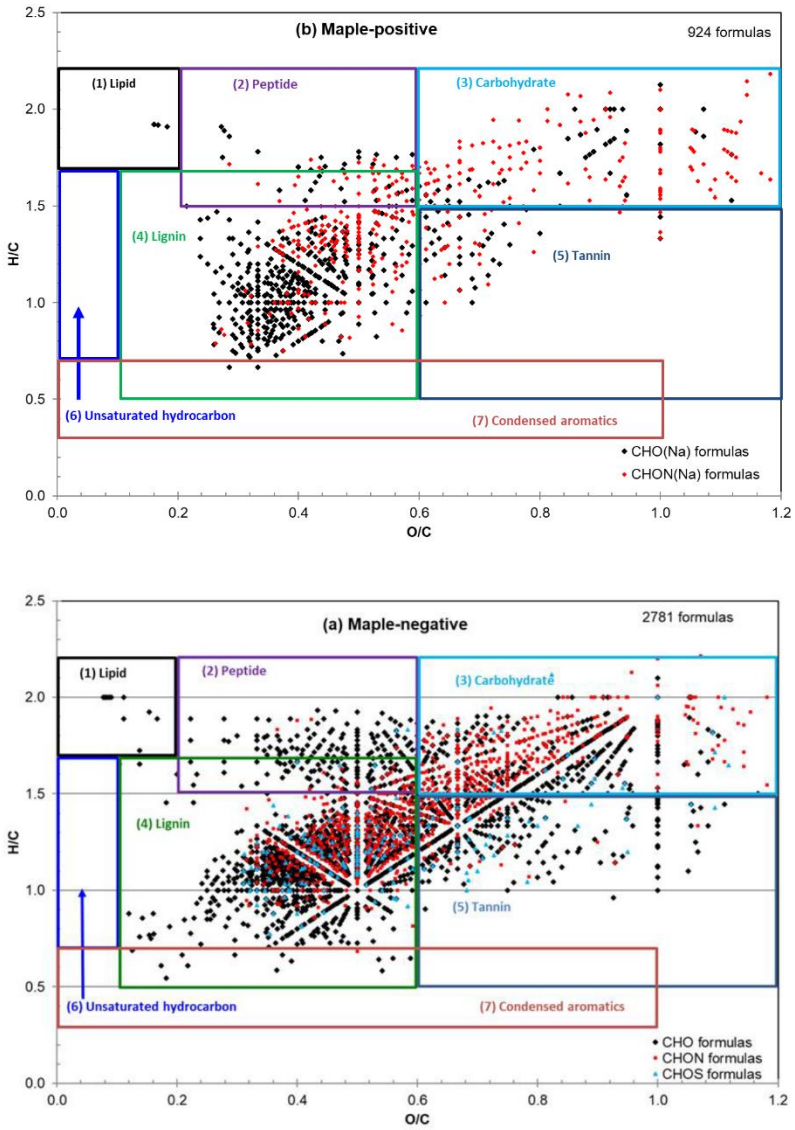

Fig. 3. The 2D van Krevelen diagrams of the maple water extractives. Overlain boxes show where the seven major biomolecular compound classes align.

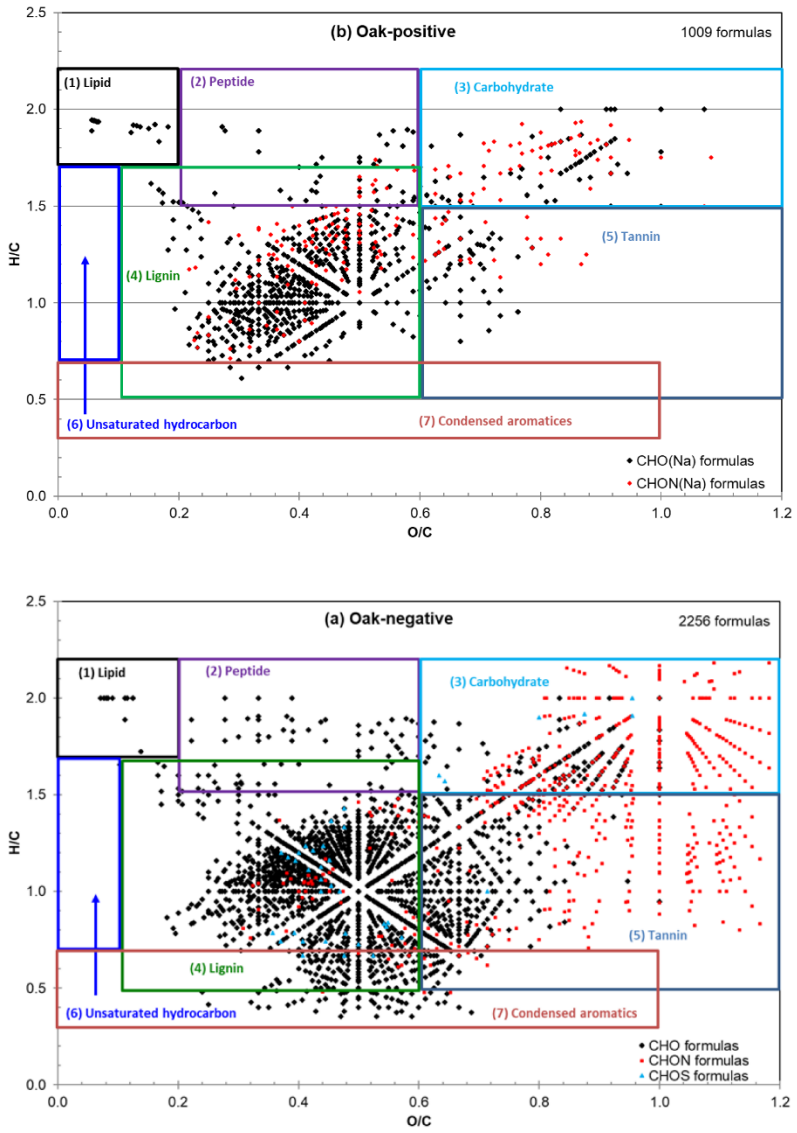

Fig. 4. The 2D van Krevelen diagrams of the oak water extractives. Overlain boxes show where the seven major biomolecular compound classes align.

Table 1. Yield and UV-vis parameters of maple and oak water extractives. Absorbance values (A_{250} and A_{365}) were with 1/100x (I), 1/50x (II), 1/20x (III), or 1/10x (IV) diluted extractives for the E2/E3 values. A_{400} and A_{600} were with undiluted extractives for the E4/E6 values. Data are presented with averages ± standard deviations (n=3).

	Yield (%)	A_{250}	A_{365}	E2/E3	A_{400}	A_{600}	E4/E6
Maple	3.14 ± 0.04	0.102 ± 0.021 II	0.020 ± 0.005 II	5.18 ± 0.25	0.404 ± 0.004	0.057 ± 0.003	7.15 ± 0.41
		0.496 ± 0.015 IV	0.077 ± 0.001 IV	6.42 ± 0.15			
Oak	2.87 ± 0.07	0.410 ± 0.026 I	0.024 ± 0.002 I	17.34 ± 0.11	0.829 ± 0.078	0.060 ± 0.020	14.52 ± 3.12
		2.150 ± 0.165 III	0.128 ± 0.011 III	16.86 ± 0.78			

Table 2. Total number of assigned formulas and selected average FT-ICR-MS peak parameters.

Sample	Formula	Number Averages				
		m/z	C	O/C	H/C	DBE
Maple, negative	2781	546	24.4	0.57	1.35	9.5
Maple, positive	924	477	21.3	0.53	1.31	9.1
Oak, negative	2256	534	23.9	0.59	1.17	11.6
Oak, positive	1009	457	21.6	0.47	1.24	9.6
Bio-oil-o, negative [a]	1926	490	29.4	0.14	1.55	8.4
Bio-oil-o, positive [a]	2000	425	25.6	0.09	1.52	8.4
Plant WEOM, negative [b]	882	431	22.7	0.36	1.50	7.38
Soil MHA, negative [b]	701	420	23.6	0.33	1.34	9.16

[a]: Bio-oil oily fraction from defatted cottonseed meal; data related to [19].

[b]: Water extracted organic matter (WEOM) of plant biomass, and soil mobile humic acid (MHA). Data were adopted from [59].

C is the number of carbons in the assigned formulas

O/C is the atomic ratio of oxygen to carbon

H/C is the atomic ratio of hydrogen to carbon

DBE (double bond equivalents) = (2c + 2 + n + p - h)/2 for any molecular formula $C_cH_hN_nO_oS_sP_p$

Table 3. The percentage of formulas (by number, num, and by peak magnitude, mag) of the types of formulas assigned in the wood extractives.

Sample	%CHO (Na)		%CHON (Na)		%CHOS (Na)	
	num	mag	num	mag	num	mag
Maple-negative	63%	75%	31%	18%	6%	7%
Maple-positive	60%	82%	40%	18%	0%	0%
Oak-negative	75%	83%	23%	16%	2%	1%
Oak-positive	81%	86%	19%	14%	0%	0%

Na was only included in positive ion mode

Table 4. Diversity (the number and % of formulas) and relative abundance (% of the total spectral magnitude) of the biomolecular compound classes in the water extractives of maple and oak, as identified by negative and positive ion mode ESI-FT-ICR-MS.

Class	**Definition**	**Amount**	**Maple-negative**	**Maple-positive**	**Oak-negative**	**Oak-positive**
Lipid	O/C 0.0-0.2 H/C 1.7-2.2	Number	10	4	11	16
		% Form.	0.4%	0.4%	0.5%	1.6%
		% Mag.	0.1%	0.1%	0.1%	0.5%
Peptide	O/C 0.2-0.6 H/C 1.5-2.2 N/C>0.05	Number	19	25	0	7
		% Form.	0.7%	2.7%	0%	1%
		% Mag.	0.1%	0.8%	0%	0%
Carbohydrate	O/C 0.6-1.2 H/C 1.5-2.2	Number	614	177	356	114
		% Form.	22%	19%	16%	11%
		% Mag.	39%	24%	22%	8%
Lignin	O/C 0.1-0.6 H/C 0.5-1.7 AI<0.67	Number	1600	610	1199	752
		% Form.	58%	66%	53%	75%
		% Mag.	51%	35%	59%	81%
Tannin	O/C 0.6-1.2 H/C 0.5-1.5 AI<0.67	Number	436	89	535	93
		% Form.	16%	10%	24%	9%
		% Mag.	9%	39%	14%	8%
Unsaturated hydrocarbon	O/C 0.0-0.1 H/C 0.7-1.7	Number	0	0	0	0
		% Form.	0%	0%	0%	0%
		% Mag.	0%	0%	0%	0%
Condensed aromatics	O/C 0.0-1.0 H/C 0.3-0.7 AI>0.67	Number	5	0	115	2
		% Form.	0.18%	0.00%	5%	0%
		% Mag.	0.03%	0.00%	2%	0%
Extra [a]	--	Number	97	19	40	25
		% Form.	3%	2%	2%	2%
		% Mag.	1%	2%	3%	1%
Total # Formulas	--	--	2781	924	2256	1009

[a]: Compounds that do not fit into any of the above categories

% form = % of the total number of formulas

% mag = % of the total spectral magnitudeextractives. The peaks in red font are those found in the top 25 peaks of more than one spectrum of the maple and oak extractives. Formulas in black, dark blue, light blue, and pink are CHO, CHON, CHONa, and CHOS, respectively.

Table 5. Relative abundances (% of total spectral magnitude), formulas, double bond equivalents (DBE), and compound class of the top 25 peaks detected in the FT-ICR mass spectra of the maple extractives. The peaks in red font are those found in the top 25 peaks of more than one spectrum of the maple and oak extractives. Formulas in black, dark blue, light blue, and pink are CHO, CHON, CHONa, and CHOS, respectively.

Maple-negative						Maple-positive					
MS peak (m/z)	Exact Mass	Height (%)	Formula	DBE	Class	MS peak (m/z)	Exact Mass	Height (%)	Formula	DBE	Class
341.1087	341.1089	13.590	$C_{12}H_{21}O_{11}$	2	Carb	381.0792	381.0792	30.690	$C_{15}H_{18}O_{10}Na$	7	Lignin
683.2246	683.2251	7.167	$C_{24}H_{43}O_{22}$	3	Carb	365.1053	365.1054	9.513	$C_{12}H_{22}O_{11}Na$	2	Carb
529.1580	529.1576	4.604	$C_{24}H_{25}O_{10}N_4$	14	Lignin	385.0894	385.0894	4.031	$C_{18}H_{18}O_8Na$	10	Lignin
585.2340	585.2341	2.760	$C_{31}H_{37}O_{11}$	13	Lignin	355.0789	355.0788	3.013	$C_{17}H_{16}O_7Na$	10	Lignin
503.1617	503.1618	2.011	$C_{18}H_{31}O_{16}$	3	Carb	360.1500	360.1500	2.017	$C_{12}H_{26}O_{11}N$	1	Carb
555.1177	555.1178	1.906	$C_{24}H_{27}O_{16}S$	11	Lignin	325.1129	325.1129	1.571	$C_{12}H_{21}O_{10}$	3	Carb
567.2082	567.2083	1.478	$C_7H_{35}O_{13}$	10	Lignin	381.0773	381.0776	1.268	$C_{12}H_{17}O_{12}N_2$	6	Tannin
577.0872	577.0869	1.344	$C_{22}H_{25}O_{16}S$	10	Tannin	543.1321	543.132	1.209	$C_{21}H_{28}O_{15}Na$	8	Tannin
665.2145	665.2146	1.300	$C_{24}H_{41}O_{21}$	4	Carb	366.1087	366.1084	1.022	$C_9H16O_5N_3$	14	Lignin
443.1922	443.1923	1.288	$C_{21}H_{31}O_{10}$	6	Tannin	459.1262	459.1262	0.865	$C_{21}H_{24}O_{10}Na$	10	Lignin
555.2235	555.2236	1.214	$C_{30}H_{35}O_{10}$	13	Lignin	503.1677	503.1676	0.850	$C_{27}H_{28}O_8Na$	14	Lignin
605.1933	605.1935	1.106	$C_{22}H_{37}O_{19}$	4	Carb	425.1571	425.1571	0.838	$C_{22}H_{26}O_7Na$	10	Lignin
583.2183	583.2185	0.966	$C_{31}H_{35}O_{11}$	14	Lignin	517.1317	517.1316	0.675	$C_{23}H_{26}O_{12}Na$	11	Lignin
379.0826	379.0823	0.879	$C_{21}H_{15}O_7$	14	Lignin	339.1050	339.1050	0.673	$C_{14}H_{20}O_8Na$	5	Lignin
497.1124	497.1123	0.763	$C_{22}H_{25}O_{11}S$	10	Lignin	428.1762	428.1763	0.672	$C_{16}H_{20}O_12N$	3	Carb
479.1195	479.1195	0.680	$C_{22}H_{23}O_{12}$	11	Lignin	369.1156	369.1156	0.648	$C_{15}H_{22}O_9Na$	5	Lignin
671.2040	671.2040	0.630	$C_{26}H_{39}O_{20}$	7	Tannin	383.0836	383.0834	0.630	$C_{14}H_{15}O_9N_4$	10	Tannin
571.182	571.1821	0.520	$C_{29}H_{31}O_{12}$	14	Lignin	527.1582	527.1583	0.599	$C_{18}H_{32}O_{16}Na$	3	Carb

617.224	617.224	0.513	$C_{31}H_{37}O_{13}$	13	Lignin	386.0928	386.0929	0.530	$C_{12}H_{20}O_{13}N$	4	Carb
533.1723	533.1723	0.436	$C_{19}H_{33}O_{17}$	3	Carb	455.1161	455.1160	0.464	$C_{18}H_{24}O_{12}Na$	7	Tannin
534.1828	534.1828	0.422	$C_{22}H_{32}O_{14}N$	7	Tannin	356.0823	356.0824	0.415	$C_{11}H_{18}O_{12}N$	4	Carb
613.2289	613.2290	0.418	$C_{32}H_{37}O_{12}$	14	Lignin	457.1470	457.1469	0.412	$C_{22}H_{26}O_{9}Na$	10	Lignin
515.1922	515.1923	0.393	$C_{27}H_{31}O_{10}$	12	Lignin	385.0875	385.0878	0.389	$C_{15}H_{17}O_{1}0N_{2}$	9	Tannin
587.2134	587.2134	0.372	$C_{30}H_{35}O_{12}$	13	Lignin	499.1364	499.1363	0.388	$C_{27}H_{24}O_{8}Na$	16	Lignin
691.2110	691.2104	0.368	$C_{30}H_{35}O_{15}N_{4}$	15	Lignin	487.1938	487.1938	0.369	$C_{24}H_{32}O_{9}Na$	9	Lignin
	Total	47.128					Total	63.751			

Table 6. Relative abundances (% of total spectral magnitude), formulas, double bond equivalents (DBE), and compound class of the top 25 peaks detected in the FT-ICR mass spectra of the oak extractives. The peaks in red font are those found in the top 25 peaks of more than one spectrum of the maple and oak extractives. Formulas in black, dark blue, light blue, and pink are CHO, CHON, CHONa, and CHOS, respectively.

Oak-negative						Oak-positive					
MS peak (m/z)	Exact Mass	Height (%)	Formula	DBE	Class	MS peak (m/z)	Exact Mass	Height (%)	Formula	DBE	Class
419.1708	419.1711	14.172	$C_{22}H_{27}O_8$	9	Lignin	459.1413	459.1414	9.783	$C_{25}H_{24}O_7Na$	14	Lignin
487.182	487.1821	6.744	$C_{22}H_{31}O_{12}$	7	Lignin	457.1258	457.1258	2.799	$C_{25}H_{22}O_7Na$	15	Lignin
605.1932	605.1935	5.726	$C_{22}H_{37}O_{19}$	4	Carb	401.1593	401.1595	2.367	$C_{22}H_{23}O_7$	11	Lignin
581.2239	581.2240	3.815	$C_{28}H_{37}O_{13}$	10	Lignin	443.1675	443.1676	2.111	$C_{22}H_{28}O_8Na$	9	Lignin
481.2291	481.2290	1.735	$C_{21}H_{37}O_{12}$	3	Lignin	460.1448	460.145	1.951	$C_{19}H_{26}O_{12}N$	8	Tannin
551.2134	551.2134	1.413	$C_{27}H_{35}O_{12}$	10	Lignin	419.1699	419.1700	1.766	$C_{22}H_{27}O_8$	10	Lignin
481.0625	481.0624	1.390	$C_{20}H_{17}O_{14}$	12	Tannin	473.1207	473.1207	1.097	$C_{25}H_{22}O_8Na$	15	Lignin
461.0725	461.0725	0.801	$C_{21}H_{17}O_{12}$	13	Lignin	459.1389	459.1398	0.988	$C_{22}H2_3O_9N_2$	13	Lignin
641.1685	641.1683	0.771	$C_{23}H_{33}O_{19}N_2$	8	Tannin	367.1209	367.1211	0.983	$C_{12}H_{24}O_{11}Na$	1	Carb
377.0878	377.0878	0.755	$C_{18}H_{17}O_9$	10	Lignin	399.1203	399.1203	0.897	$C_{23}H_{20}O_5Na$	14	Lignin
447.0569	447.0569	0.754	$C_{20}H_{15}O_{12}$	13	Lignin	435.1648	435.165	0.803	$C_{22}H_{27}O_9$	10	Lignin
603.1779	603.1778	0.723	$C_{22}H_{35}O_{19}$	5	Carb	351.1260	351.1262	0.791	$C_{12}H_{24}O_{10}Na$	1	Carb
461.1301	461.1301	0.661	$C_{19}H_{25}O_{13}$	7	Tannin	417.0945	417.0945	0.754	$C_{22}H_{18}O_7Na$	14	Lignin
565.1369	565.1370	0.590	$C_{17}H_{29}O_{19}N_2$	4	Carb	441.1518	441.152	0.645	$C_{22}H_{26}O_8Na$	10	Lignin
471.1355	471.1355	0.580	$C_{17}H_{27}O_{15}$	4	Carb	375.1414	375.1414	0.629	$C_{18}H_{24}O_7Na$	7	Lignin

300.9989	300.9990	0.571	$C_{14}H_5O_8$	12	Lignin	419.1101	419.1101	0.600	$C_{22}H_{20}O_7Na$	13	Lignin
611.1943	611.1941	0.544	$C_{23}H_{35}O_{17}N_2$	7	Carb	457.1469	457.1469	0.552	$C_{22}H_{26}O_9Na$	10	Lignin
329.2333	329.2333	0.523	$C_{18}H_{33}O_5$	2	Extra	461.1396	461.1402	0.548	$C_{18}H_{25}O_{12}N_2$	8	Tannin
449.1261	449.1260	0.490	$C_{13}H_{25}O_{15}N_2$	2	Carb	433.0894	433.0894	0.532	$C_{22}H_{18}O_8Na$	14	Lignin
537.1423	537.1421	0.485	$C_{16}H_{29}O_{18}N_2$	3	Carb	444.1709	444.1712	0.528	$C_{16}H_{30}O_{13}N$	3	Carb
535.1264	535.1264	0.479	$C_{16}H_{27}O_{18}N_2$	4	Carb	402.1627	402.1636	0.510	$C_{18}H_{25}O_6N_3Na$	8	Lignin
571.1820	571.1821	0.390	$C_{29}H_{31}O_{12}$	14	Lignin	507.1263	507.1262	0.496	$C_{25}H_{24}O_{10}Na$	14	Tannin
515.1921	515.1923	0.369	$C_{27}H_{31}O_{10}$	12	Lignin	417.1543	417.1544	0.479	$C_{22}H_{25}O_8$	11	Lignin
605.2238	605.2240	0.360	$C_{30}H_{37}O_{13}$	12	Lignin	621.1944	621.1942	0.465	$C_{31}H_{34}O_{12}Na$	15	Lignin
575.2134	575.2134	0.336	$C_{29}H_{35}O_{12}$	12	Lignin	481.1856	481.1857	0.448	$C_{27}H_{29}O_8$	14	Lignin
	Total	45.177					Total	33.523			